Published in: Biochemical Journal (2008), vol. 414, iss.1, pp.151-159
Status: Posprint (Author's version)

Mutational analysis of the zinc- and substrate-binding sites in the CphA metallo-*β*-lactamase from *Aeromonas hydrophila*

Carine BEBRONE*[1], Christine ANNE*[1], Frédéric KERFF*, Gianpiero GARAU†, Kris DE VRIENDT‡, Raphaël LANTIN*, Bart DEVREESE‡, Jozef VAN BEEUMEN‡, Otto DIDEBERG†, Jean-Marie FRERE* and Moreno GALLENI*

**Centre d'Ingénierie des Protéines, Université de Liège, Allée du 6 Août B6, Sart-Tilman 4000 Liège, Belgium, † Institut de Biologie Structurale Jean-Pierre Ebel (CNRS-CEA-UJF), rue Jules Horowitz 41, 38027 Grenoble Cedex 1, France, and ‡Laboratorium voor Eiwitbiochemie en Eiwitengineering, K.L. Ledeganckstraat 35, University of Gent, B-9000 Gent, Belgium*

Abstract: The subclass B2 CphA (Carbapenemase hydrolysing *Aeromonas)* *β*-lactamase from *Aeromonas hydrophila* is a Zn^{2+} -containing enzyme that specifically hydrolyses carbapenems. In an effort to evaluate residues potentially involved in metal binding and/or catalysis (His^{118}, Asp^{120}, His^{196} and His^{263}) and in substrate specificity (Val^{67}, Thr^{157}, Lys^{224} and Lys^{226}), site-directed mutants of CphA were generated and characterized. Our results confirm that the first zinc ion is in interaction with Asp^{120} and His^{263}, and thus is located in the 'cysteine' zinc-binding site. His^{118} and His^{196} residues seem to be interacting with the second zinc ion, as their replacement by alanine residues has a negative effect on the affinity for this second metal ion. Val^{67} plays a significant role in the binding of biapenem and benzylpenicillin. The properties of a mutant with a five residue (LFKHV) insertion just after Val^{67} also reveals the importance of this region for substrate binding. This latter mutant has a higher affinity for the second zinc ion than wild-type CphA. The T157A mutant exhibits a significantly modified activity spectrum. Analysis of the K224Q and N116H/N220G/K224Q mutants suggests a significant role for Lys^{224} in the binding of substrate. Lys^{226} is not essential for the binding and hydrolysis of substrates. Thus the present paper helps to elucidate the position of the second zinc ion, which was controversial, and to identify residues important for substrate binding.

Keywords: *β*-lactamase, carbapenem, enzymatic kinetics, site-directed mutagenesis, substrate binding, zinc-binding site.

INTRODUCTION

In vivo, class B *β*-lactamases [1] require one or two zinc ions as enzymatic cofactors. By efficiently catalysing the hydrolysis of the *β*-lactam amide bond, these enzymes play a key role in bacterial resistance to this group of antibiotics. Several pathogens are now known to synthesize members of this class [2-7]. Metallo-*β*-lactamases exhibit very broad activity spectra [8]. Moreover, they are not susceptible to the common *β*-lactamase inactivators [9]. Presently, no clinically efficient inhibitor of metallo-*β*-lactamases has been found. The fact that some of the metallo-*β* -lactamase genes are plasmid-encoded represents an additional cause for concern [10,11]. On the basis of the known metallo-*β*-lactamase sequences, three different lineages, identified as subclasses B1, B2 and B3, can be characterized [12,13]. The enzymes exhibit two potential zinc-binding sites containing His^{116} (Asn^{116} in subclass B2), His^{118} and His^{196} in subclasses B1 and B3; and Asp^{120}, Cys^{221} (His^{121} in subclass B3) and His^{263} in subclasses B1 and B2. Each subclass thus possesses a different set of potential zinc ligands.

The CphA (Carbapenemase hydrolysing *Aeromonas)* metallo-*β* -lactamase produced by *Aeromonas hydrophila* belongs to subclass B2, which is characterized by a uniquely narrow specificity profile. In contrast with metallo-*β*-lactamases of subclasses Bl and B3, CphA efficiently hydrolyses only carbapenems and displays very poor activity against penicillins and cephalosporins [8,14], and exhibits maximum activity as a mono-zinc enzyme. The presence of a Zn^{2+} ion in a second low-affinity binding site noncompetitively inhibits the enzyme with a K_i value of 46 μM at pH 6.5 [15]. The structure of the mono-zinc CphA enzyme has been solved by X-ray crystallography [16]. Similarly to the known structures of metallo-*β*-lactamases of subclasses Bl [17-22] and B3 [23,24], the X-ray structure of CphA reveals an *αββα* sandwich, with two central *β*-sheets and α-helices on the external faces. The active site is located at the bottom of the *β* -sheet core. In contrast with all reported structures

Abbreviations used: CphA, Carbapenemase hydrolysing *Aeromonas;* ESI, electrospray ionization; ICP-MS, inductively coupled plasma MS; LB, Luria-Bertani.

[1] These authors contributed equally to this work.

Published in: Biochemical Journal (2008), vol. 414, iss.1, pp.151-159
Status: Posprint (Author's version)

for the Bl and B3 subclasses, a long α3 helix (Arg^{140}-Leu^{161}) is located near the active-site groove of CphA. This α3 helix is a key element of the 'hydrophobic wall' which defines the active-site pocket. Thus whereas the enzymes of subclasses B1 and B3 exhibit a large cavity, the active site of CphA is very well defined and this explains the very narrow activity profile of the enzyme [16].

Contrary to the enzymes of subclasses Bl and B3, it was demonstrated that, in the subclass B2 CphA enzyme, a cysteine residue contributes to the first catalytic zinc-binding site [16,25-27]. This result suggested that the respective binding sites of the first and second zinc ions would be reversed in CphA compared with Bl and B3 metallo-*β*-lactamases. However, on the basis of spectroscopic studies with another subclass B2 enzyme (ImiS), Crowder and co-workers postulate that the second zinc-binding site is not the traditional 'histidine' site, but involves both His^{118} and Met^{146} [28,29].

Furthermore, by soaking CphA crystals in a biapenem solution, a reaction intermediate could be trapped into the active site of the enzyme [16]. The analysis of this structure allowed us to select several residues potentially important for substrate binding such as Val^{67}, Thr^{157}, Lys^{224} and Lys^{226} (Figure 1).

The side chain of Val^{67} is in van der Waals contact with the 1*β*-methyl group of biapenem. Val^{67} is a residue of the L1 loop (Tyr^{60}-Val^{67}) [13,16] and is part of the 'hydrophobic wall' which defines the active site of CphA. The Val^{67} residue is conserved in the B2 subclass metallo-*β*-lactamases and in the BcII, CcrA and IMP-1 Bl subclass enzymes [13]. The hydroxyl group of Thr^{157} forms hydrogen bonds with the hydroxyethyl group on C-6 of biapenem and, after hydrolysis, with the newly formed carboxylate group [16]. Thr^{157}, a residue of the α3 helix located near the active-site groove, is only conserved in subclass B2 enzymes. As in CcrA and IMP-1 subclass Bl enzymes [21,30-33], the side chain of Lys^{224} forms an electrostatic interaction with the invariant carboxylate group on C-3 of *β*-lactam. It is conserved in subclass B2 and B1 enzymes, with the exception of VIM-2 [13]. The Lys^{226} side chain is the only charged side chain near the C-2 bicyclotriazoliumthio group of biapenem.

Figure 1 : *Structure of biapenem (a), the reaction intermediate (b) and view of the active site of CphA in complex with the reaction intermediate (c)*

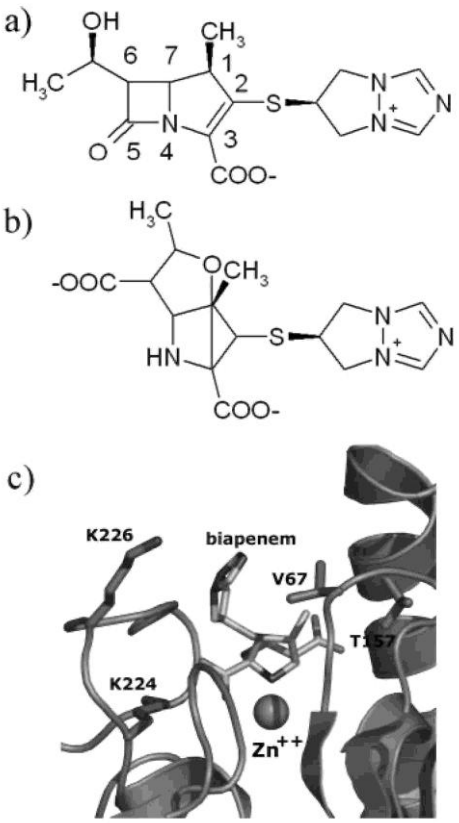

In order to evaluate their importance in metal binding and/or catalysis, substitutions of residues potentially involved in zinc binding have been performed by site-directed mutagenesis (H118A, D120A, D120T, H196A

and H263A). To examine the effects of the charge or size of the residues on the substrate specificity, Val^{67} was replaced by an alanine, isoleucine or aspartic acid residue, Thr^{157} by an alanine residue, and Lys^{224} and Lys^{226} by glutamine residues. Lys^{224} was also replaced by a glutamine residue in the Nl 16H/N220G extended-spectrum double mutant [34].

EXPERIMENTAL

Bacterial strains and vectors

Escherichia coli DH5α (Stratagene) and *E. coli* BL21 (DE3) pLysS Star (Invitrogen) strains were used as hosts for the construction of the different expression vectors and for the production of *β*-lactamases respectively. pET9a-CphA [35] was used as the plasmid template for PCR site-directed mutagenesis amplifications. The pK18-CphA vector was constructed by ligation of the EcoRI/SmaI excised fragment of pAS20R [4] and the SmaI/ HindIII excised fragment of pET9a-CphA [35] into the polylinker of the pK18 vector at the EcoRI and HindIII sites [36]. Moreover, a unique PstI restriction site was introduced by site-directed mutagenesis at the end of the signal-peptide coding sequence. The CphAPstIa and CphAPstIb primers used for this purpose are described in Supplementary Table S1 (at http://www. BiochemJ.org/bj/414/bj4140151add.htm). pK18-CphA was then used as the DNA template in the pentapeptide scanning reaction [37] described below.

Chemicals and antibiotics

The primers used for the mutagenesis were synthesized by Eurogentec (Liège, Belgium). Kanamycin was purchased from Merck. Imipenem ($\Delta\varepsilon_{300}$ = - 9000 M^{-1} . cm^{-1}) was from Merck Sharp and Dohme and biapenem ($\Delta\varepsilon_{294}$ = - 9900 M^{-1} . cm^{-1}) was from Shionogi Pharmaceutical (Osaka, Japan). Ampicillin, benzylpenicillin ($\Delta\varepsilon_{235}$ = - 775 M^{-1} . cm^{-1}), cephaloridine ($\Delta\varepsilon_{260}$ = - 10000 M^{-1} . cm^{-1}) and cefotaxime ($\Delta\varepsilon_{260}$ = - 7500 M^{-1} . cm^{-1}) were purchased from Sigma, and nitrocefin ($\Delta\varepsilon_{482}$ = -15000M^{-1} . cm^{-1}) from Unipath Oxoid (Basingstoke, U.K.). The variations of the molar extinction coefficients on *β*-lactam hydrolysis are from references [38] (biapenem) and [39]. The antibiotics used in this study are illustrated in Figure 1 (biapenem) and Supplementary Figure S1 (at http://www.BiochemJ. org/bj/414/bj414015 ladd.htm).

Site-directed mutagenesis

The QuikChange® site-directed mutagenesis kit (Stratagene) was used to generate all the mutations. The primers designed for these experiments are listed in Supplementary Table S1. The mutants were constructed using pET9a-CphA WT (where WT is wild-type) as the DNA template. The triple mutant N116H/N220G/ K224Q was constructed using the pET9a-Nl 16H-N220G mutant construct [34] as the template DNA. The introduction of the desired mutations and the absence of additional unwanted mutations were always verified by DNA sequence analysis.

Pentapeptide scanning

A pentapeptide-scanning reaction [37] was performed with the help of the GPS™-LS scanning system (New England Biolabs). This system allows the insertion of 15 bp linkers at random positions throughout the *blaCphA* gene on the pK8-CphA plasmid. The different plasmids were used to transform *E. coli* DH5α by electroporation. The colonies were selected on LB (Luria-Bertani) agar plates supplemented with 50 μg/ml kanamycin and 10 μg/ml imipenem, and 50 μg/ml kanamycin and 8 μg/ml benzylpenicillin respectively. The plasmids were prepared and the different *blaCphA* genes were DNA sequenced in order to determine the position of the insertion.

Protein expression and purification

The genes encoding the mutant proteins were cloned into pET9a using the BamHI and NdeI restriction sites. The different vectors were then introduced into *E. coli* strain BL21 (DE3) pLysS Star. Overexpression and purification of mutant proteins was performed as described previously for the wild-type protein [15,27,35] with the following modification. Bacteria expressing the wild-type protein were grown for 8 h at 37 °C in 2YT medium, whereas those expressing the mutant proteins were grown for 24 h at 18 °C in the same medium. Growth at this reduced temperature was made necessary by the fact that the mutant proteins were produced mainly in a non-soluble form (inclusion bodies) when the cultures were grown at 37 °C.

Published in: Biochemical Journal (2008), vol. 414, iss.1, pp.151-159
Status: Posprint (Author's version)

ESI (electrospray ionization)-MS and metal content determination

Samples of wild-type and mutant CphA enzymes were equilibrated in 10 mM ammonium acetate buffer (pH 6.5) by centrifugal filtration prior to ESI-MS. For each protein, mass spectra were obtained under both denaturing and native conditions. Denaturation of the protein was performed by dilution of the protein to a final concentration of 2-5 μM in 1:1 (v/v) water/acetonitrile containing 0.1 % formic acid. The native protein was diluted to 10-15 μM in 10 mM ammonium acetate buffer.

All mass spectra were acquired on a Q-TOF1 mass spectrometer (Micromass) equipped with a nano ESI source using Au/Pd-coated borosilicate needles purchased from Protana (Odense, Denmark). Capillary voltage was set at 1250 V and cone voltage at 40 V and 60 V for the denatured and native proteins respectively. Acquisition time was 3 to 5 min across an *m/z* range of 400-3000. The mass spectra were processed with MassLynx v3.1 software (Micromass). The instrument was calibrated using a mixture of myoglobin and trypsinogen. The zinc content of each protein was derived from the mass difference between the native and denatured proteins.

Determination of the zinc content using ICP-MS (inductively coupled plasma MS)

Protein samples were dialysed against 15 mM sodium cacodylate (pH 6.5). Protein concentrations were determined by measuring the absorbance at 280 nm (ε_{280} = 38500 M^{-1} cm^{-1}). The zinc content was determined by ICP-MS as described previously [15, 27].

Stability toward chaotropic agents

The stability of the different proteins was studied by fluorescence. The wild-type and mutant enzymes (0.05 mg/ml) were incubated for 16 h in the presence of increasing urea concentrations (0-8 M) at 4 °C. Fluorescence emission spectra of the enzymes were recorded at 20 °C with a PerkinElmer LS50B luminescence spectrometer using excitation and emission wavelengths of 280 and 333 nm respectively.

CD

CD spectra of the different enzymes (0.5 mg/ml) were obtained using a JASCO J-810 spectropolarimeter. The spectra were scanned at 20 °C from 200 to 250 nm (far-UV) and from 250 to 310 nm (near-UV) with 1 nm steps.

Determination of kinetic parameters

Hydrolysis of the antibiotics was monitored by following the absorbance variation resulting from the opening of the β -lactam ring, using a Uvikon 860 spectrophotometer equipped with thermostatically controlled cells and connected to a microcomputer. For biapenem, imipenem, benzylpenicillin, nitrocefin, cephaloridine and cefotaxime, the wavelengths measured were 294, 300, 235, 482, 260 and 260 nm respectively. Cells with 0.2-1.0 cm pathlengths were used, depending on the substrate concentrations. When the K_m values of the studied enzymes were sufficiently high, the k_{cat} and K_m parameters were determined either under initial-rate conditions, using the Hanes linearization of the Henri-Michaelis-Menten equation, or by analysing the complete hydrolysis time courses [40]. Low and very high K_m values were determined as K_i values using imipenem or nitrocefin as reporter substrates. In the cases of low K_m values, the k_{cat} values were obtained from the initial hydrolysis rates measured at saturating substrate concentration and, in the cases of high K_m values, k_{cat} was derived from the k_{cat}/K_m ratio. All experiments were performed at 30 °C in 15 mM sodium cacodylate (pH 6.5).

Inactivation by EDTA

Inactivation of CphA wild-type and the H118A, H196A, H263A and D120A mutants by EDTA was studied in 15 mM sodium cacodylate (pH 6.5) at 30 °C in the presence of different concentrations of EDTA in a total volume of 0.5 ml. Imipenem (200 μM) was used as the reporter substrate. Since the inactivation time courses followed pseudo-first-order kinetics, the rate constants characterizing the inactivation of the enzyme were calculated from the dependence of the pseudo-first-order constant K_i on the chelating agent concentration on the basis of the following model:

$$\mathrm{E.Zn} + \mathrm{C} \overset{K}{\rightleftarrows} \mathrm{E.Zn.C} \underset{k_{-2}}{\overset{k_{+2}}{\rightleftarrows}} \mathrm{E} + \mathrm{Zn.C}$$

where C is the chelator, E is the apoenzyme, E.Zn is the metalloenzyme, E.Zn.C is a ternary metalloenzyme-chelator complex, k_{+2} is the individual rate constant for the dissociation of E.Zn.C into E + Zn.C, k_{-2} is the association constant, which was negligible in the case of the H263A mutant, K is the dissociation constant of the E.Zn.C ternary complex and Zn.C is the metal-chelator complex.

As [Zn.C] is higher than [E], the ternary complex formation from the apoenzyme and the zinc-chelator complex is characterized by a pseudo-first-order constant: $k_{-2}' = k_{-2}[\text{Zn.C}]$.

The individual values of K and k_{+2} were determined by fitting the values of K_i to eqn (1):

$$k_i = \frac{k_{+2}[C]}{K\{(K_m + [S])/K_m\} + [C]} = k_{-2} \qquad (1)$$

where [S] and K_m were the concentration and the K_m value of the reporter substrate respectively.

Enzymatic measurement in the presence of increasing concentrations of zinc and determination of K_{d2}

Residual activity in the presence of increasing concentrations of zinc was measured at 30 °C in 15 mM sodium cacodylate (pH 6.5) as already described [27]. When binding of the second zinc ion resulted in a complete loss of activity, the data were analysed according to eqn (2) [27]:

$$\text{RA} = \{K_{d2}/([\text{Zn}] + K_{d2})\} \times 100 \qquad (2)$$

where RA is the residual activity and K_{d2} is the dissociation constant for the second zinc ion.

When binding of the second zinc ion resulted in an incomplete loss of activity or in an increase of activity, the following equation was used [27]:

$$\text{RA} = \{(K_{d2} + \alpha[\text{Zn}])/([\text{Zn}] + K_{d2})\} \times 100 \qquad (3)$$

where a is the ratio of activity at saturating zinc concentration $\{[\text{Zn}]_{(\infty)}\}$ compared with activity in the absence of added zinc $\{[\text{Zn}]_{(0)}\}\{\text{activity } [\text{Zn}]_{(\infty)}/\text{activity } [\text{Zn}]_{(0)}\}$.

Experimental data were fitted to eqn (2) or eqn (3) by non-linear regression analysis using SigmaPlot software.

Published in: Biochemical Journal (2008), vol. 414, iss.1, pp.151-159
Status: Posprint (Author's version)

Table 1: *Masses and metal binding for CphA wild-type and mutant constructs measured under native and denatured conditions. The average mass of a Zn^{2+} ion is 65.4 Da. However, two or more protons can be displaced on protein binding, giving the bound Zn^{2+} ion an apparent mass of 63.4 Da.*

Protein	Assay conditions	Calculated mass (Da)	Measured mass (Da)	Mass difference (Da)	Number of Zn^{2+} ions
Wild-type	Native	-	25253.5	63.9	
	Denatured	25189	25189.6	-	-
H118A	Native	-	25187.6	62.8	
	Denatured	25123	25124.8	-	-
D120A	Native	-	25206.7	61.6	
	Denatured	25146	25145.1	-	-
D120T	Native	-	25237.3	62.2	
	Denatured	25176	25175.1	-	-
H196A	Native	-	25187.6	62.9	
	Denatured	25123	25124.7	-	-
H263A	Native	-	25218.5	62.7	
	Denatured	25123	25122.4	-	-
V67A	Native	-	25223.3	62.9	
	Denatured	25161	25160.4	-	-
V67I	Native	-	25265.1	60.8	
	Denatured	25203	25204.3	-	-
V67D	Native	-	25266.9	62.1	
	Denatured	25205	25204.8	-	-
$V67_{LFKHV}$	Native	-	25874.8	62.4	1 (70%)
	Native	-	25936.3	123.9	2 (30%)
	Denatured	25904(25815)*	25812.4	-	-
T157A	Native	-	25221.7	63.3	
	Denatured	25159	25158.4	-	-
K224Q	Native	-	25251.8	61.7	
	Denatured	25189	25190.1	-	-
K226Q	Native	-	25252.5	63.7	
	Denatured	25189	25188.8	-	-
N116H/R121H/K224Q	Native	-	25218.8	62.7	
	Denatured	25155	25156.1	-	-

*The value in parentheses is obtained by assuming the elimination of the C-terminal serine residue.

RESULTS AND DISCUSSION

A mutant protein containing an LFKHV insertion located just after Val^{67} (hereafter referred to as $V67_{LFKHV}$) was obtained by a pentapeptide-scanning experiment. The *E. coli* DH5α cells transformed by pK18-CphA $V67_{LFKHV}$ were unable to grow on LB agar plates supplemented with 10 µg/ml imipenem, in contrast with bacteria producing the wild-type enzyme. These cells were also unable to grow in the presence of 8 µg/ml ampicillin. The $V67_{LFKHV}$ mutant was produced in the periplasmic fraction of *E. coli* DH5α (result not shown).

The different mutants were expressed in *E. coli* BL21 (DE3) pLysS Star and purified to homogeneity. The presence of the mutations was verified by MS (Table 1). Within experimental errors, the mutants were found to exhibit the expected masses, with the exception of the $V67_{LFKHV}$ mutant, which presented a mass deficit of 92 Da. The N-terminal sequence of this mutant showed that there is no amino acid loss at the N-terminal side. The difference between the calculated and measured masses could thus be due to the loss of the C-terminal serine.

The stability of the different mutants in the presence of a denaturating agent (urea) was similar to that of the wild-type enzyme ($C_{1/2}$ = 2.7-3 M) except for the T157A mutant ($C_{1/2}$ = 2.2 M) and the H263A mutant ($C_{1/2}$ = 2.4 M), which were a little less stable.

All the mutant constructs had far-UV CD spectra which were superimposable on that of wild-type CphA (results not shown). The tertiary structures were conserved for the H118A and H196A mutant constructs, whereas the environment of one or more aromatic residues was modified in the H263A, D120A and D120T mutant constructs when compared with the wild-type enzyme (see Supplementary Figure S2 at http://www.BiochemJ.org/bj/414/ bj4140151add.htm). Near-UV CD spectra and fluorescence emission spectra of the N116H/N220G/K224Q and $V67_{LFKHV}$ mutant constructs suggested a small conformation change occurred in the protein tertiary structure (results not shown). Such a small conformational change had already been observed for the N116H/ N220G double mutant [34].

The activities of the mutants were measured against several compounds representing the three major families of *β*-lactam antibiotics, namely carbapenems, penicillins and cephalosporins, in the absence of added zinc (free zinc concentrations below 0.4 μM) (Tables 2 and 3). Under these conditions, all the mutant constructs, except $V67_{LFKHV}$, were shown to contain one zinc ion, as does the wild-type enzyme (Tables 1 and 4). $V67_{LFKHV}$ already exhibited a di-zinc form (30 %) in conditions where the wild-type enzyme only co-ordinates a single zinc ion (Table 1).

Mutational analysis of zinc-binding sites

Although His^{118} and His^{196} are not involved in the binding of the catalytic metal ion [16], their replacement by alanine residues drastically reduces the enzymatic activity, suggesting important roles for these residues in the catalytic mechanism. The H118A and H196A mutations lead to a decrease of at least 1000-fold in activity against carbapenems compared with the wild-type enzyme (Table 2). This result is perfectly in agreement with the structural data. Garau et al. [16] suggested that His^{118} is the general base which activates the hydrolytic water molecule and that His^{196} contributes to the oxyanion hole by forming a hydrogen bond with the carbonyl oxygen of the *β*-lactam bond. Moreover, these residues might stabilize the carboxylate which is formed on hydrolysis of the substrate. This 'active role' of His^{118} and His^{196} contrasts with the results obtained for Asn^{116}, which in subclass B2 enzymes replaces His^{116}, one of the zinc ligands for enzymes in subclasses B1 and B3. Indeed, whereas the H116S substitution reduces the activity of the subclass B1 *Bacillus cereus* enzyme 15-20-fold, the N116S substitution in CphA yielded an enzyme whose catalytic and zinc-binding properties were similar to those of the wild-type enzyme. These results indicate that Asn^{116} in subclass B2 enzymes is not a 'functional substitute' for His^{116} in subclasses Bl and B3 [27].

Table 2: *Kinetic parameters of the wild-type CphA enzyme and the H118A, H196A, H263A, D120A and D120T mutant constructs. Measurements were taken at 30°C in 15 mM sodium cacodylate (pH 6.5). Values for the wild-type enzyme are from Vanhove et al. [27]. S.D. values (not shown) were below 10%. N.D., not determined.*

Enzyme	Substrate	k_{cat} (s^{-1})	K_m (μM)	k_{cat}/K_m ($M^{-1} . s^{-1}$)
Wild-type	Imipenem	1200	340	3500000
	Biapenem	300	170	1800000
	Benzylpenicillin	0.03	870	35
	Nitrocefin	0.008	1300	6
	Cephaloridine	< 0.006	6000	<1
H118A	Imipenem	2.4	1150	2100
	Biapenem	0.1	730	150
	Benzylpenicillin	0.007	210	33
	Nitrocefin	0.005	30	170
	Cephaloridine	>0.01	>4500	2.2
H196A	Imipenem	16	4300	3700
	Biapenem	N.D.	N.D.	N.D.
	Benzylpenicillin	>0.1	>5000	20
	Nitrocefin	0.006	15	400
	Cephaloridine	> 0.11	>4500	24
H263A	Imipenem	0.02	1700	12
	Biapenem	> 0.005	>1500	3
	Benzylpenicillin	N.D.	N.D.	N.D.
	Nitrocefin	0.003	15	200
	Cephaloridine	N.D.	N.D.	N.D.
D120A	Imipenem	0.024	330	73
	Biapenem	0.0015	100	15
	Benzylpenicillin	N.D.	N.D.	N.D.
	Nitrocefin	0.0024	26	92
	Cephaloridine	N.D.	N.D.	N.D.
D120T	Imipenem	0.025	210	120
	Biapenem	N.D.	N.D.	N.D.
	Benzylpenicillin	N.D.	N.D.	N.D.
	Nitrocefin	0.0002	50	4
	Cephaloridine	N.D.	N.D.	N.D.

After replacement of Asp^{120} and His^{263} by residues which cannot serve as zinc ligands, the mutant proteins could still bind one zinc ion, but were also catalytically impaired in a dramatic manner. The D120A, D120T and H263A mutations resulted in a very large decrease in the activities against carbapenems (at least 50000-fold), mainly due to strongly decreased k_{cat} values (Table 2). This very low residual activity could be explained by a poor positioning of the Zn^{2+} ion in the active site of the mutants and a deformation of its co-ordination sphere. In this respect, it is interesting to note that the N220G mutation, which does not directly affect any of the zinc ligands but is situated next to Cys^{221}, causes a displacement of the latter in 20% of the molecules [16].

ICP-MS shows that, in contrast with the wild-type enzyme, these five mutant enzymes remain in their mono-zinc forms even in the presence of 100 μM free zinc (Table 4).

The effect of the zinc ion concentration on enzyme activity has also been studied. The binding of the second zinc ion is severely affected by the H118 A and H196A mutations (Figure 2a). From these curves, the H118A and H196A mutants are found to exhibit much higher K_{d2} values (940 ± 80 and 1250 ± 50 µM respectively) than the wild-type enzyme (46 ± 3 µM*).* The poorer binding of the second zinc ion by CphA H118A was also demonstrated by MS, which failed to detect the di-zinc form of this mutant [41]. This indicates that both histidine residues are involved in the binding of the second, inhibitory, zinc ion.

This interpretation is in disagreement with the conclusions of Crowder and co-workers that the inhibitory zinc ion binds at a distance of at least 0.5 nm from the catalytic one in the ImiS subclass B2 enzyme [28]. Our results could be reconciled with this hypothesis if both of our mutations resulted in significant conformational changes. On the basis of the CD data (Supplementary Figure S2), this does not seem to be the case. Crowder and co-workers have shown that the inhibitory zinc ion is bound by a sulphur atom [29]. The sulphur ligand in the inhibitory site should come from a methionine residue, since the only cysteine residue (Cys^{221}) is a ligand of the first zinc ion. The mutation of Met^{146} to an isoleucine residue abolishes metal inhibition. However, mutation of other CphA residues, which have not been implicated as ligands of the second zinc ion, can have similar effects (lower inhibition or even activation by an excess of zinc, as observed below). Moreover, a careful examination of the CphA three-dimensional structure indicates that His^{118} and Met^{146} are poorly positioned to bind the same zinc ion. The distance between their Cα groups is 7.57 Å (1 Å = 0.1 nm), whereas the distances between the sulphur atom of Met^{146} and the nitrogen atoms of the imidazole group of His^{118} are 10.40 and 10.91 Å respectively. Also, the space between these residues does not allow the accommodation of a zinc ion because it is occupied by the backbone of the Asn^{114}-His^{118} loop connecting strand $\beta 6$ and helix α2.

Moreover, the involvement of His^{118} and His^{196} in the binding of the inhibitory zinc ion makes sense in the light of the strongly decreased activity of the mutants (Table 2), since this binding would prevent them from playing their catalytic roles in the hydrolysis of carbapenems.

According to the structure, the presence of a second zinc ion in the active site interacting with His^{118} and His^{196} would not require any major rearrangement. There is indeed a free space between those residues and Cys^{221}, Asp^{120} and Asn^{116}. This second zinc ion would approximately be located at a position similar to that of the first zinc ion in subclasses B1 and B3 β-lactamases and two of the zinc ligands would be conserved. Compared with the available structure of CphA, the only modification needed would be a 180° rotation around the Cβ-Cγ bond of the His^{196} side chain to bring the Nε2 atom into the required orientation (Figure 3).

Published in: Biochemical Journal (2008), vol. 414, iss.1, pp.151-159
Status: Posprint (Author's version)

Table 3: *Kinetic parameters of the CphA wild-type, V67A, V67I, V67D, V67$_{LFKHV}$, T157A, K224Q, K226Q, N116H/N220G and N116H/N220G/K224Q mutant enzymes. Measurements were performed at 30°C in 15 mM sodium cacodylate (pH 6.5). Values for the wild-type enzyme are from Vanhove et al. [27] and values for the N116H/N220G double mutant are from Bebrone et al. [34]. S.D. values (not shown) are below 10%.*

Enzyme	Antibiotics	k_{cat} (s^{-1})	K_m (µM)	k_{cat}/K_m ($M^{-1} . s^{-1}$)
Wild-type	Imipenem	1200	340	3500000
	Biapenem	300	170	1800000
	Benzylpenicillin	0.03	870	35
	Nitrocefin	0.008	1300	6
	Cefotaxime	> 0.0002	>100	2
V67A	Imipenem	1000	220	4500000
	Biapenem	100	100	1000000
	Benzylpenicillin	0.004	1000	4
	Nitrocefin	0.005	26	180
V67I	Imipenem	1770	180	9000000
	Biapenem	>50	>1500	33000
	Benzylpenicillin	0.08	730	110
	Nitrocefin	0.004	50	80
V67D	Imipenem	1280	310	4000000
	Biapenem	>100	>1500	66000
	Benzylpenicillin	>0.03	>5000	6
	Nitrocefin	0.004	36	110
V67LFKHV	Imipenem	>30	>1500	20000
	Biapenem	>2.4	>1500	1600
	Nitrocefin	> 0.006	>2000	3
T157A	Imipenem	1680	570	3000000
	Biapenem	>130	>1500	87000
	Benzylpenicillin	1	550	1950
	Nitrocefin	0.015	110	140
	Cefotaxime	0.023	450	50
K224Q	Imipenem	>490	>1500	330000
	Biapenem	>60	>1500	40000
	Benzylpenicillin	>0.03	>5000	6
	Nitrocefin	0.007	135	52
	Cephaloridine	0.024	1000	24
	Cefotaxime	0.001	700	1.4
K226Q	Imipenem	1000	380	2600000
	Biapenem	1000	840	1200000
	Benzylpenicillin	0.004	800	5
	Nitrocefin	0.01	850	12
	Cephaloridine	0.006	1700	3.5
	Cefotaxime	0.0006	140	4.3
N116H/N220G	Imipenem	16	185	86000
	Biapenem	5	100	50000
	Benzylpenicillin	3.3	150	22000
	Nitrocefin	0.7	4	180000
	Cephaloridine	0.9	145	6200
	Cefotaxime	0.3	50	6000
N116H/N220G/K224Q	Imipenem	0.9	300	3000
	Biapenem	0.26	390	670
	Benzylpenicillin	0.13	920	140
	Nitrocefin	0.2	32	6000
	Cephaloridine	0.03	53	570
	Cefotaxime	0.015	434	34

Published in: Biochemical Journal (2008), vol. 414, iss.1, pp.151-159
Status: Posprint (Author's version)

Table 4: Summary of zinc binding for CphAwild-type and the H118A, H196A, H263A, D120A and D120T mutants. *S.D. values (not shown) were below 10%. N.D., not determined.*

	$[Zn^{2+}] \leq 0.4\mu M$		$[Zn^{2+}] = 100\mu M$	
Protein	MS	ICP-MS	MS	ICP-MS
Wild-type	1	1.0	2	1.9
H118A	1	0.9	N.D.	1.2
H196A	1	N.D.	N.D.	1.2
H263A	1	1.0	N.D.	0.9
D120A	1	1.3	N.D.	1.3
D120T	1	1.3	N.D.	1.3

From this crude modelling, the identity of the third ligand of the second zinc ion is not clear. However, the fact that Cys^{221} CphA mutants no longer bind zinc [27], whereas mutants of the two other ligands (Asp^{120} and His^{263}) of the first zinc-binding site retain relatively high affinities for zinc (K_d < 0.4 μM) points towards a role of Cys^{221} in the binding of both zinc ions. The role of a cysteine residue in the simultaneous binding of two zinc ions is a known feature that has been observed previously; for example, in the structure of the DNA-binding domain of the Gal4 transcription factor [42]. The second zinc-binding site described here would probably be more energetically favourable (one side chain rotation) than the major rearrangement required to organize a zinc-binding site involving the embedded Met^{146} residue. The presence of a sulphur atom in the second binding site that resulted in the identification of Met^{146} could maybe be explained by the involvement of Cys^{221} in the binding of both ions.

Figure 2: *Percentage residual activity measured in the presence of increasing concentrations of zinc.* ***(a)*** *CphA wild-type (WT, •) and the H118A (A) and H196A (■) mutants activity on imipenem. The curves are the best fits determined using eqn (2). (b) CphA WT (•) and the D120A (Δ), D120T (□) and H263A (♦) mutants activity on imipenem. The curves are the best fits determined using eqn (2). All experiments were performed at 30°C in 15 mM sodium cacodylate (pH 6.5) with a substrate concentration of 100 μU. S.D. values (not shown) are below 10%.*

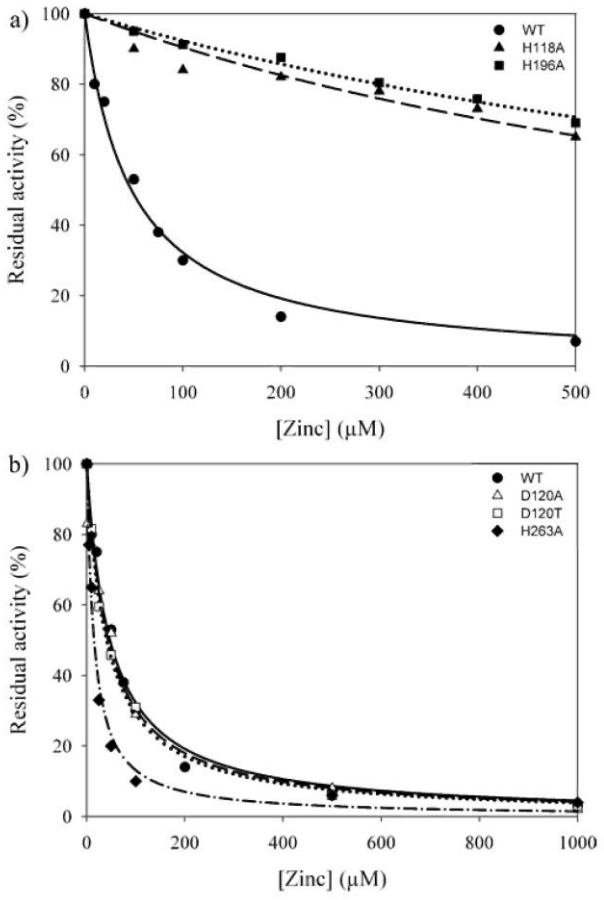

The affinities of the Asp[120] and His[263] mutant constructs are nonetheless probably decreased when compared with that of the wild-type enzyme, as indicated by higher rates of inactivation by EDTA (Table 5). The rates of inactivation are probably between those observed for site 1 and site 2 in the wild-type enzyme, for which the K_{dl} is below 10 pM [43] and K_{d2} is 46 μM [15]. Because the residual activity of these mutants can be inhibited by EDTA and because the K_{d2}' values deduced from the inhibition by zinc are still relatively close to 46 μM (Figure 2b) {K_{d2} values arel5±1.5µMforH263Aand44±6and41±2µMforD120A and D120T mutants respectively), the binding of the first zinc ion to these mutants might result from a reduced affinity for site 1 rather than an improved affinity for the inhibitory site 2. The occupation of both sites at the same time has not been observed [41].

Mutational analysis of putative substrate-binding-site residues

Our kinetic results are in good agreement with the crystallographic structure of CphA in complex with biapenem [16] and confirm the importance of the Val[67] residue for the binding of this substrate into the active site of CphA. The K_m values of the V67I and V67D mutants for biapenem strongly increase in comparison with wild-type CphA, so that only k_{cat}/K_m could be measured (Table 3). This phenomenon could be due to a less favourable interaction with the 1β-methyl group of the antibiotic. In addition, we show that a hydrophobic interaction between Val[67] and the C-2 methyl groups of penicillin is likely, since the K_m value of the V67D mutant construct for benzylpenicillin is larger than that of the wild-type CphA enzyme (Table 3). A similar interaction has already been proposed between the BcII subclass B1 enzyme and benzylpenicillin [44]. Moreover, Simona et al. [45] have recently suggested a possible role of the L1 loop (Tyr[60]-Val[67]) in the mechanism of binding carbapenem molecules.

Figure 3: *Representation of the active site of the CphA enzyme.*
(a) *Structure of the mono-zinc active site (PDB code 1X8G). (b) Model of a di-zinc active site with addition of a zinc ion and rotation of the His[196] side chain, the only modification when compared with (a). The dashed lines show bonds to atoms within 3 Å of the second zinc ion (Zn2).*

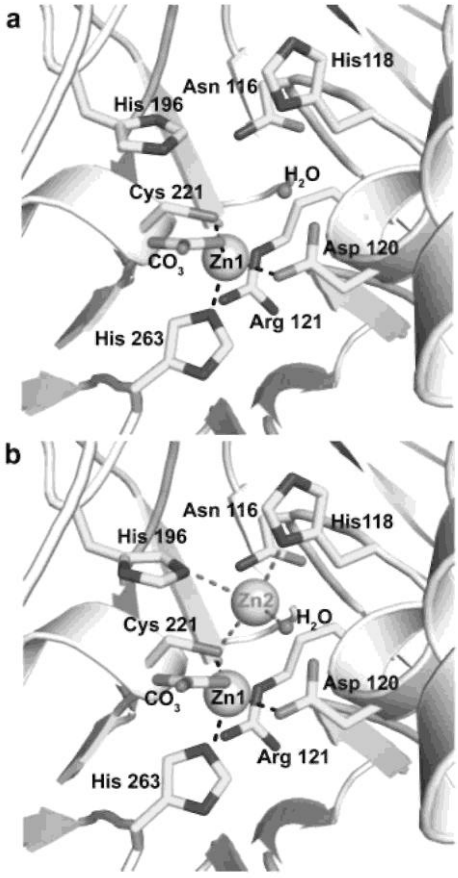

Table 5: *Individual parameters for the inactivation of CphA wild-type, H118A, H196A, H263A and D120A mutant constructs by EDTA. S.D. values (not shown) were below 10%.*

Protein	*K*(mM)	k_{+2}(s^{-1})	k_{-2}(s^{-1})	k_{+2}/K($M^{-1}.s^{-1}$)
Wild-type	5.5	0.007	0.0014	1.3
H118A	5.2	0.002	0.003	0.4
H196A	16.4	0.008	0.005	0.5
H263A	0.01	0.005	-	500
D120A	0.5	0.003	0.00001	6

As for wild-type CphA [15], the binding of a second zinc ion inhibits the hydrolysis of imipenem by the Val^{67} mutants in a noncompetitive manner. The dissociation constants for the second zinc ion are similar to that of the wild-type enzyme for the V67I and V67D mutants (46 ± 3 µM*)* or slightly reduced for the V67A mutant (16 + 3 µM*).*

The $V67_{LFKHV}$ mutant, with a five-residue insertion just after Val^{67}, displays a strongly decreased affinity for biapenem, imipenem and nitrocefin (Table 3). The extended loop might fold above the active-site groove and in this way reduce the accessibility of the active site. The lengthening of the L1 loop and/or the introduction of a charged residue (lysine) could have a negative effect on the affinity of the enzyme for its substrate. The apparent dissociation constant for the second zinc ion is below 1 *µM,* whereas it is 46 *µM* for wild-type CphA. Together with the fact that this mutant exhibits a di-zinc form (30 %) under conditions where the wild-type enzyme is only mono-zinc, this result suggests that the histidine residue in the inserted pentapep-tide might probably interact with the second zinc ion, thus recreating a possible second 'three histidine' zinc-binding site (His^{67}-His^{118}-His^{196}). However, a significant rearrangement would be necessary in order to bring the additional histidine residue into sufficiently close proximity to His^{118} and His^{196}. Consequently, this hypothesis should be confirmed by EXAFS and PAC (perturbed angular correlation) experiments and by resolution of the three-dimensional structure.

Various modifications can broaden the activity spectrum of the strict CphA carbapenemase. The N116H/N220G extended-spectrum mutant was obtained by a site-directed approach on the basis of sequence alignments between members of the B2 and B1 subclasses [34]. In the present paper, surprisingly, the replacement of Thr^{157} with an alanine residue results in a significant modification of the activity spectrum of the enzyme, since the catalytic efficiency of this mutant towards benzylpenicillin, cefotaxime and nitrocefin is larger than that of the wild-type enzyme. However, although the T157A mutant is far from being as efficient as the N116H/N220G mutant [34], it retains, in contrast, strong activity towards imipenem (Table 3).

Thr^{157} does not seem to play an important role in the CphA catalytic mechanism, but according to the structure of CphA in complex with modified biapenem (PDB code 1X81) and the proposed mechanism for enzymatic activity on carbapenems [16], the C-6 (C-7 for cephalosporins) side chains of *β*-lactam antibiotics are likely to be located in the environment of Thr^{157} during hydrolysis. A residue with a slightly reduced bulkiness could therefore be more suited to accommodate the larger and differently oriented side chain of most *β*-lactam antibiotics compared with carbapenems. This could explain the more extended spectrum observed for this mutant. Because the T157A mutant only retains a good activity against imipenem whereas the interactions of imipenem and biapenem with Thr^{157} should be affected similarly, we believe that this residue is more important for optimum positioning of the substrate than for its affinity for the active site. The bulkier and more rigid biapenem would therefore need extra anchoring to be perfectly oriented, whereas imipenem would fit more naturally into the active site.

Zinc ions inhibit the hydrolysis of imipenem and benzylpenicillin by the T157A mutant in a non-competitive manner, but the di-zinc form of this mutant retains 40 % activity towards benzylpenicillin, whereas it is practically completely deprived of activity towards imipenem (Figure 4a). The dissociation constants for the second zinc ion are similar for both substrates and similar to that of the wild-type enzyme (46 ± 3 µM for T157A and imipenem, 55 ± 11 µM for T157A and benzylpenicillin and 46 ± 3 µM for the wild-type enzyme and imipenem [15] respectively).

Published in: Biochemical Journal (2008), vol. 414, iss.1, pp.151-159
Status: Posprint (Author's version)

Figure 4: *Percentage residual (or relative) activity measured in the presence of increasing concentrations of zinc. (a) T157A mutant construct incubated with imipenem and benzylpenicillin. The curves are the best fits determined using eqn (2) (●, imipenem) or eqn (3) (A, benzylpenicillin).*
(b) N116H/N220G/K224Q triple mutant incubated with imipenem and nitrocefin. The curves are the best fits determined using eqn 3 (●, imipenem; ■ nitrocefin). All experiments were performed at 30°C in 15 mM sodium cacodylate (pH 6.5). The substrate concentrations were 100 µM for imipenem, 1 mM for benzylpenicillin and 100 µM for nitrocefin. S.D. values (not shown) are below 10%.

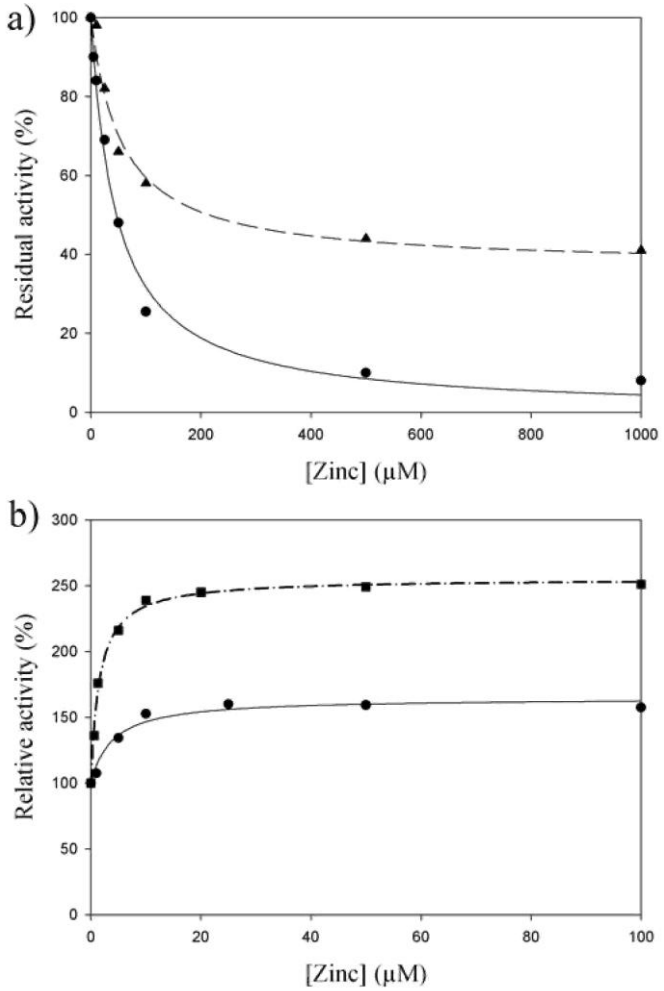

In contrast with the N116H/N220G mutant [34], imipenem and benzylpenicillin seem in this case to be hydrolysed via the same mechanism. The activity of wild-type CphA against benzylpenicillin is too low to allow meaningful measurements to be obtained; however, zinc also behaves as an inhibitor in this case.

Our kinetic results show that Lys^{224} is important for the binding of *β*-lactam antibiotics into the active site of CphA, as already observed for the subclass B1 enzymes CcrA and IMP-1 [21,30-33]. The K224Q mutant exhibits a decreased catalytic efficiency towards carbapenem substrates when compared with the wild-type enzyme. The individual k_{cat} and K_m values could not be determined. In the same way, the K_m value for benzylpenicillin is strongly increased (Table 3). This role is in good agreement with the crystallographic structure of CphA in complex with biapenem, which shows an electrostatic interaction between Lys^{224} and the invariant C-3 carboxylate of the *β*-lactam antibiotic, and with the simulations of Xu et al. [46].

The N116H/N220G/K224Q triple mutant presents increased K_m values and decreased k_{cat} values when compared with the Nl16H/N220G double mutant (Table 3). This triple mutant, while significantly less active than the N116H/N220G double mutant, retains a relatively extended spectrum when compared with the wild-type enzyme. It is particularly interesting since, as already observed for the N116H/R121H/N220G triple mutant [34] and in contrast with the wild-type enzyme, added zinc acts as an activator. The hydrolysis rate of imipenem and nitrocefin by the N116H/N220G/K224Q triple mutant strikingly increases to 1.6- and 2.5-fold respectively at

saturating Zn^{2+} concentrations (Figure 4b). The dissociation constant for the second zinc ion determined for this triple mutant (4.0 ± 1.1 μM and 1.6 ± 0.2 μM with imipenem and nitrocefin respectively as substrates) is similar to that of the Nl 16H/N220G double mutant (5.0 ± 0.9 μM [34]). For all of the other mutants, the hydrolysis of nitrocefin is independent of the concentration of zinc.

This phenomenon remains difficult to explain in the absence of structural data on the di-zinc-inhibited form of the wild-type enzyme, but it is quite likely that binding of the second zinc ion induces distinct structural changes in both the wild-type and mutant proteins.

The replacement of Lys^{226} only affects the kinetic parameters of biapenem. Although the k_{cat} value is increased, the catalytic efficiency remains similar to that of the wild-type enzyme. The K226Q mutation does not significantly modify the affinity for the second zinc ion (K_{d2} = 85±10μM).

Conclusion

Our results indicate that His^{118} and His^{196} participate in the catalytic mechanism of the subclass B2 CphA metallo-*β*-lactamase, for which an intact Asp^{120}/Cys^{221}/His^{263} site is essential. The position of the second inhibitory zinc ion has not been identified with certainty, but it is likely to be equivalent to the 'histidine' site observed in subclass B1 and B3 enzymes. His^{118} and His^{196} are involved in the binding of this second zinc ion and Cys^{221} is the leading candidate as the third ligand, but the geometry is perhaps sub-optimal and Asn^{116} or Asp^{120} could play a role also.

The present paper underlines the importance of Val^{67}, Thr^{157} and Lys^{224} residues for carbapenem binding into the active site of CphA.

Acknowledgments

This work was supported by the Belgian Federal Government (PAI P5/33), grants from the FNRS [(Fonds de la Recherche Scientifique), Brussels, Belgium; FRFC grants 24508.01, 2.4.524.03 and Loterie Nationale 9.4538.03] and by the European Research Training Network (MEBEL contract HPTR-CT-2002-00264). The purchase of a Jasco J-810 spectropolarimeter was supported in part by a grant from the FRFC (contract number 2.4545.01). C.B. and F.K. were FNRS post-doctoral researchers, and C.A. was the recipient of a Marie Curie fellowship.

REFERENCES

1 Ambler, R. P. (1980) The structure of *β*-lactamases. Philos. Trans. R. Soc. London Ser. B 289, 321-331

2 Rasmussen, B. A., Gluzman, Y and Tally, F. P. (1990) Cloning and sequencing of the class B *β*-lactamase gene (ccrA) from *Bacteroides fragilis* TAL3636. Antimicrob. Agents Chemother. 34,1590-1592

3 Watanabe, M., lyobe, S., Inoue, M. and Mitsuhashi, S. (1991) Transferable imipenem resistance in *Pseudomonas aeruginosa.* Antimicrob. Agents Chemother. 35,147-151

4 Massidda, O., Rossolini, G. M. and Satta, G. (1991) The *Aeromonas hydrophila* cphA gene: molecular heterogeneity among class B metallo-*β*-lactamases. J. Bacteriol. 173, 4611-4617

5 Osano, E., Arakawa, Y, Wacharotayankun, R., Ohta, M., Horii, T, Ito, PL, Yoshimura, F. and Kato, N. (1994) Molecular characterization of an enterobacterial metallo *β*-lactamase found in a clinical isolate of *Serratia marcescens* that shows imipenem resistance. Antimicrob. Agents Chemother. 38, 71-78

6 Rossolini, G. M., Franceschini, N., Riccio, M. L, Mercuri, P. S., Perilli, M., Galleni, M., Frère, J. M. and Amicosante, G. (1998) Characterization and sequence of the *Chryseobacterium (Flavobacterium) meningosepticum* carbapenemase: a new molecular class B *β*-lactamase showing a broad substrate profile. Biochem. J. 332,145-152

7 Chen, Y, Succi, J., Tenover, F. C. and Koehler, T. M. (2003) *β*-Lactamase genes of the penicillin-susceptible *Bacillus anthracis* Sterne strain. J. Bacteriol. 185, 823-830

8 Felici, A., Amicosante, G., Oratore, A., Strom, R., Ledent, P., Joris, B., Fanuel, L. and Frère, J. M. (1993) An overview of the kinetic parameters of class B *β*-lactamases. Biochem. J. 291,151-155

9 Prosperi-Meys, C, Llabres, G., de Seny, D., Soto, R. P., Valladares, M. H., Laraki, N., Frère, J. M. and Galleni, M. (1999) Interaction between class B *β*-lactamases and suicide substrates of active-site serine *β*-lactamases. FEBS Lett. 443,109-111

10 Livermore, D. M. and Woodford, N. (2000) Carbapenemases: a problem in waiting? Curr. Opin. Microbiol. 3, 489-495

11 Walsh, T. R., Toleman, M. A., Poirel, L. and Nordmann, P. (2005) Metallo-*β*-lactamases: the quiet before the storm. Clin. Microbiol. Rev. 18, 306-325

12 Galleni, M., Lamotte-Brasseur, J., Rossolini, G. M., Spencer, J., Dideberg, O., Frère, J. M. and the Metallo-*β*-lactamases Working Group (2001) Standard numbering scheme for class B β-lactamases. Antimicrob. Agents Chemother. 45, 660-663

13 Garau, G., Garcia-Saez, I., Bebrone, C, Anne, C, Mercuri, P. S., Galleni, M., Frère, J. M. and Dideberg, 0. (2004) Update of the standard numbering scheme for class B *β*-lactamases. Antimicrob. Agents Chemother. 48, 2347-2349

14 Segatore, B., Massida, O., Satta, G., Setacci, D. and Amicosante, G. (1993) High specificity of CphA-encoded metallo-*β*-lactamase from *Aeromonas hydrophila* AE036 for carbapenems and its contribution to *β*-lactam resistance. Antimicrob. Agents Chemother. 37, 1324-1328

15 Hernandez-Valladares, M., Felici, A., Weber, G., Adolph, H. W., Zeppezauer, M., Rossolini, G. M., Amicosante, G., Frère, J. M. and Galleni, M. (1997) Zn(ll) dependence of the *Aeromonas hydrophila* AE036 metallo-*β*-lactamase activity and stability. Biochemistry 36, 11534-11541

16 Garau, G., Bebrone, C, Anne, C, Galleni, M., Frère, J. M. and Dideberg, 0. (2005) A metallo-*β*-lactamase enzyme in action: crystal structures of the monozinc carbapenemase CphA and its complex with biapenem. J. Mol. Biol. 345, 785-795

17 Carfi, A, Pares, S,, Duee, E,, Galleni, M,, Duez, C, Frère, J. M. and Dideberg, 0. (1995) The 3-D structure of a zinc metallo-*β*-lactamase from *Bacillus cereus* reveals a new type of protein fold. EMBO J. 14, 4914-4921

18 Concha, N. O., Rasmussen, B. A, Bush, K. and Herzberg, 0. (1996) Crystal structure of the wide-spectrum binuclear zinc *β*-lactamase from *Bacteroides fragilis.* Structure 4, 823-836

19 Carfi, A, Duée, E., Galleni, M., Frère, J. M. and Dideberg, 0. (1998) 1.85 Å resolution structure of the zinc (II) *β*-lactamase from *Bacillus cereus.* Acta. Cryst. D Biol. Crystallogr. 54,313-323

20 Fabiane, S. M,, Sohi, M. K,, Wan, T., Payne, D. J,, Bateson, J. H,, Mitchell, T. and Sutton, B. J. (1998) Crystal structure of the zinc-dependent *β*-lactamase from *Bacillus cereus* at 1.9 Å resolution: binuclear active site with features of a mononuclear enzyme. Biochemistry 37, 12404-12411

21 Concha, N. 0., Janson, C. A, Rowling, P., Pearson, S., Cheever, C. A, Clarke, B. P., Lewis, C, Galleni, M., Frère, J. M., Payne, D. J. et al. (2000) Crystal structure of the IMP-1 metallo *β*-lactamase from *Pseudomonas aeruginosa* and its complex with a mercaptocarboxylate inhibitor: binding determinants of a potent, broad-spectrum inhibitor. Biochemistry 39, 4288-4298

22 Garcia-Saez, I., Hopkins, J., Papamicael, C, Franceschini, N, Amicosante, G., Rossoloni, G. M., Galleni, M., Frère, J. M. and Dideberg, 0. (2003) The 1.5 Å structure of *Chryseobacterium meningosepticum* zinc *β*-lactamase in complex with the inhibitor, D-captopril. J. Biol. Chem. 278, 23868-23873

23 Ullah, J. H,, Walsh, T. R., Taylor, I. A., Emery, D. C, Verma, C. S,, Gamblin, S. J. and Spencer, J. (1998) The crystal structure of the L1 metallo-*β*-lactamase from *Stenotrophomonas maltophilia* at 1.7 Å resolution. J. Mol. Biol. 284,125-136

24 Garcia-Saez, I., Mercuri, PS., Papamicael, C, Kahn, R., Frère, J.M., Galleni, M., Rossoloni, G.M. and Dideberg, 0. (2003b) Three-dimensional structure of FEZ-1, a monomeric subclass B3 metallo-*β*-lactamase from *Fluoribacter gormanii,* in native form and in complex with D-captopril. J. Mol. Biol. 325, 651-660

25 Hernandez-Valladares, M., Kiefer, M., Heinz, U., Paul Soto, R., Meyer-Klaucke, W., Friederich Nolting, H, Zeppezauer, M., Galleni, M., Frère, J. M., Rossolini, G. M., Amicosante, G. and Adolph, H. W. (2000) Kinetic and spectroscopic characterization of native and metal-substituted *β*-lactamase from *Aemmonas hydmphila* AE036. FEBS Lett. 467, 221-225

26 Heinz, U, Bauer, R., Wommer, S, Meyer-Klaucke, W., Papamichaels, C, Bateson, J. and Adolph, H. W. (2003) Coordination geometries of metal ions in D- or L-captopril-inhibited metallo-*β*-lactamases. J. Biol. Chem. 278,20659-20666

27 Vanhove, M., Zakhem, M., Devreese, B., Franceschini, N., Anne, C, Bebrone, C, Amicosante, G., Rossolini, G. M., Van Beeumen, J., Frère, J. M. and Galleni, M. (2003) Role of Cys221 and Asn116 in the zinc-binding sites of the *Aemmonas hydmphila* metallo-*β*-lactamase. Cell. Mol. Life Sci. 60, 2501-2509

28 Crawford, P. A, Yang, K. W,, Sharma, N,, Bennett, B. and Crowder, M. W. (2005) Spectroscopic studies on cobalt(ll)-substituted metallo-*β*-lactamase ImiS from *Aemmonas veroniibv. sobria.* Biochemistry 44, 5168-5176

29 Costello, A. L, Sharma, N. P., Yang, K. W,, Crowder, M. W. and Tierney D. L. (2006) X-ray absorption spectroscopy of the zinc-binding sites in the class B2 metallo-*β*-lactamase ImiS from *Aeromonas veronii* bv. *sobria.* Biochemistry 45, 13650-13658

30 Yang, Y, Keeney D., Tang, X., Canfield, N. and Rasmussen, B. A. (1999) Kinetic properties and metal content of the metallo-*β*-lactamase CcrA harboring selective amino acid substitutions. J. Biol. Chem. 274,15706-15711

31 Yanchak, M. P., Taylor, R. A. and Crowder, M. W. (2000) Mutational analysis of metallo-*β*-lactamase CcrA from *Bacteroides fragilis.* Biochemistry 39, 11330-11339

32 Haruta, S., Yamamoto, E. T, Eriguchi, Y and Sawai, T. (2001) Characterization of the active-site residues asparagine 167 and lysine 161 of the IMP-1 metallo-*β*-lactamase. FEMS Microbiol. Lett. 197, 85-89

33 Materon, I. C, Beharry Z., Huang, W., Perez, C. and Palzkill, T. (2004) Analysis of the context dependent sequence requirements of active site residues in the metallo-*β*-lactamase IMP-1. J. Mol. Biol. 344, 653-663

34 Bebrone, C, Anne, C, De Vriendt, K., Devresse, B., Van Beeumen, J., Frère, J. M. and Galleni, M. (2005) Dramatic broadening of the substrate profile of the *Aemmonas hydmphila* CphA metallo-*β*-lactamase by site-directed mutagenesis. J. Biol. Chem. 17, 180-188

35 Hernandez-Valladares, M., Galleni, M., Frère, J. M., Felici, A., Perilli, M., Franceschini, N., Rossolini, G. M., Oratore, A. and Amicosante, G. (1996) Overproduction and purification of the *Aemmonas hydmphila* CphA metallo-*β*-lactamase expressed in *Escherichia coli.* Microb. Drug Resist. 2, 253-256

36 Pridmore, R. D. (1987) New and versatile cloning vectors with kanamycin-resistance marker. Gene 56, 309-312

37 Hallet, B., Sherrat, D. J. and Hayes, F (1997) Pentapeptide scanning mutagenesis: random insertion of a variable five amino acid cassette in a target protein. Nucleic Acids Res. 25,1866-1867

38 Mercuri, P. S., Garcia-Saez, L, De Vriendt, K, Thamm, I., Devreese, B., Van Beeumen, J., Dideberg, O., Rossolini, G. M., Frère, J. M. and Galleni, M. (2004) Probing the specificity of the sub-class B3 FEZ-1 metallo-*β*-lactamase by site-directed mutagenesis. J. Biol. Chem. 279, 33630-33638

39 Matagne, A., Dubus, A., Galleni, M. and Frère, J. M. (1999) The *β*-lactamase cycle: a tale of selective pressure and bacterial ingenuity. Nat. Prod. Rep. 16, 1-19

40 De Meester, F, Joris, B., Reckinger, G., Bellefroid-Bourguignon, C, Frère, J. M. and Waley S. G. (1987) Automated analysis of enzyme inactivation phenomena. Application to *β*-lactamases and DD-peptidases. Biochem. Pharmacol. 36, 2393-2403

41 De Vriendt, K., Van Driessche, G., Devreese, B., Bebrone, C, Anne, C, Frère, J. M., Galleni, M. and Van Beeumen, J. (2006) Monitoring the zinc affinity of the metallo-*β*-lactamase CphA by automated nanoESI-MS. J. Am. Soc. Mass Spectrom. 17, 180-188

42 Baleja, J. D., Thanabal, V and Wagner, G. (1997) Refined solution structure of the DNA-binding domain of GAL4 and use of 3J(113Cd,1H) in structure determination. J. Biomol. NMR 10, 397-401

43 Wommer, S., Rival, S., Heinz, U., Galleni, M., Frère, J. M., Franceschini, N., Amicosante, G., Rasmussen, B., Bauer, R. and Adolph, H. W. (2002) Substrate-activated zinc binding of metallo-*β*-lactamases: physiological importance of mononuclear enzymes. J. Biol. Chem. 277, 24142-24147

44 Prosperi-Meys, C, de Seny, D., Llabres, G., Galleni, M. and Lamotte-Brasseur, J. (2002) Active-site mutants of class B *β*-lactamases: substrate binding and mechanistic study. Cell. Mol. Life Sci. 59, 2136-2143

45 Simona, F, Magistrato, A, Vera, D. M. A., Garau, G., Vila, A. J. and Carloni, P. (2007) Protonation state and substrate binding to B2 metallo-*β*-lactamase CphA from *Aemmonas hydmphila.* Proteins 69,595-605

46 Xu, D., Xie, D. and Guo, H. (2006) Catalytic mechanism of class B2 metallo-*β*-lactamase. J. Biol. Chem. 281,8740-8747

Published in: Biochemical Journal (2008), vol. 414, iss.1, pp.151-159
Status: Posprint (Author's version)

SUPPLEMENTARY ONLINE DATA

Mutational analysis of the zinc- and substrate-binding sites in the CphA metallo-*β*-lactamase from *Aeromonas hydrophila*

Carine BEBRONE*[1], Christine ANNE*[1], Frédéric KERFF*, Gianpiero GARAU†, Kris DE VRIENDT‡, Raphaël LANTIN*, Bart DEVREESE‡, Jozef VAN BEEUMEN‡, Otto DIDEBERG†, Jean-Marie FRERE* and Moreno GALLENI*[2]

**Centre d'Ingénierie des Protéines, Université de Liège, Allée du 6 Août B6, Sart-Tilman 4000 Liège, Belgium, † Institut de Biologie Structurale Jean-Pierre Ebel (CNRS-CEA-UJF), rue Jules Horowitz 41, 38027 Grenoble Cedex 1, France, and ‡Laboratorium voor Eiwitbiochemie en Eiwitengineering, K.L. Ledeganckstraat 35, University of Gent, B-9000 Gent, Belgium*

Figure S1: *Structures of the β-lactam antibiotics used in this study.*
(a) *Imipenem, (b) benzylpenicillin, (c) nitrocefin, (d) cephaloridine and (e) cefotaxime.*

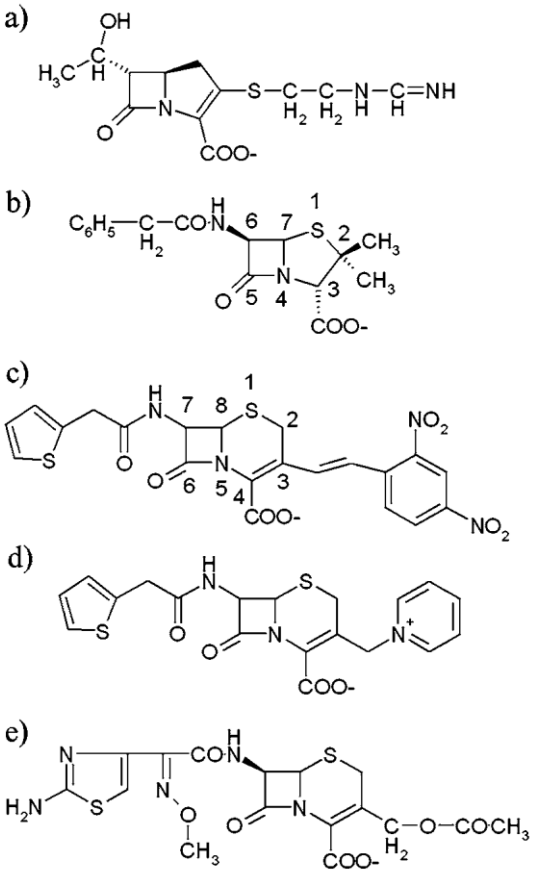

Published in: Biochemical Journal (2008), vol. 414, iss.1, pp.151-159
Status: Posprint (Author's version)

Figure S2: *Near-UV CD spectra. The protein concentrations were 0.5 mg/ml in all cases. (a) Wild-type CphA enzyme (solid line) and the H118A (dashed line) and H196A (dotted line) mutant constructs. (b) Wild-type CphA enzyme (solid line) and the D120A (dashed line), D120T (dotted line) and H263A (dashed and dotted line) mutant constructs. mdeg, degrees . cm^2 . $dmol^{-1}$.*

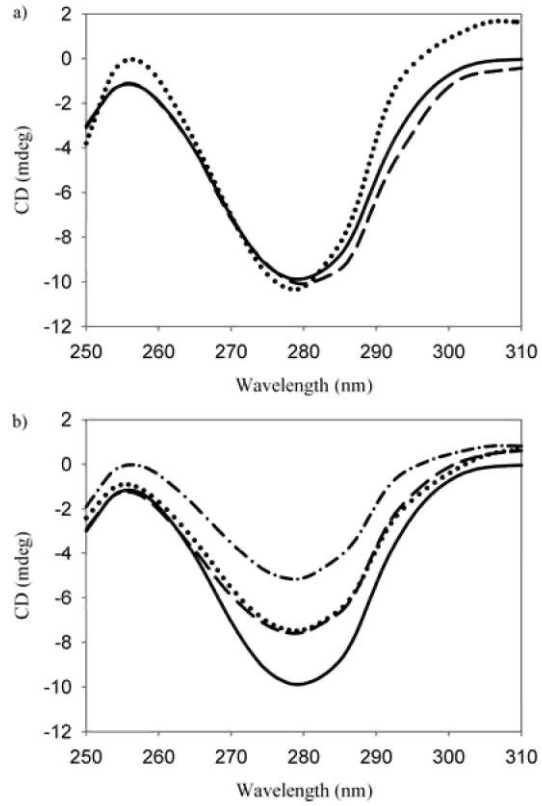

Published in: Biochemical Journal (2008), vol. 414, iss.1, pp.151-159
Status: Posprint (Author's version)

Table S1: *List of mutagenic primers used for site-directed mutagenesis. The modified bases are underlined, for, forward primer; rev, reverse primer; T_m, melting temperature (°C), Trip., triple mutant primer.*

Primers	Sequences (5' → 3')	τ_m
H118Afor	GGTGATCAACACCAACTACGCCACCGACCGGGCTGGC	83.8
H118Arev	GCCAGCCCGGTCGGTGGCGTAGTTGGTGTTGATCACC	83.8
H196Afor	CGCGGGCCCGGCCGCTACGCCGGACGGC	86.1
H196Arev	GCCGTCCGGCGTAGCGGCCGGGCCCGCG	86.1
H263Afor	GGTGATCGGCGGTGCCGACTCACCGCTGC	80.0
H263Arev	GCAGCGGTGAGTCGGCACCGCCGATCACC	80.0
D120Afor	CAACTACCACACCGCCCGGGCTGGCGG	82.4
D120Arev	CCGCCAGCCCGGGCGGTGTGGTAGTTG	82.4
D120Tfor	CCAACTACCACACCACCCGGGCTGGCGG	78.9
D120Trev	CCGCCAGCCCGGGTGGTGTGGTAGTTGG	78.9
V67Afor	AGAGGACAACTACTACGCGCAGGAAAATTCCATGG	78.9
V67Arev	CCATGGAATTTTCCTGCGCGTAGTAGTTGTCCTCT	78.9
V67Dfor	GGTAGAGGACAACTACTACGACCAGGAAAATTCCATGGTC	78.6
V67Drev	GACCATGGAATTTTCCTGGTCGTAGTAGTTGTCCTCTACC	78.6
V67lfor	GGTAGAGGACAACTACTACATCCAGGAAAATTCCATGGTC	77.6
V67lrev	GACCATGGAATTTTCCTGGATGTAGTAGTTGTCCTCTACC	77.6
T157Afor	GAGATTGTTGCCTTTGCCCGCAAGGGGC	77.8
T157Arev	GCCCCTTGCGGGCAAAGGCAACAATCTC	77.8
K224Qfor	GCAACTGCATTCTCCAGGAGAAGCTGGGC	76.8
K224Qrev	GCCCAGCTTCTCCTGGAGAATGCAGTTGC	76.8
K226Qfor	GCATTCTCAAGGAGCAGCTGGGCAACCTG	78.2
K226Qrev	CAGGTTGCCCAGCTGCTCCTTGAGAATGC	78.2
Trip.K224Qfor	GCGGCTGCATTCTCCAGGAGAAGCTGGGC	81.0
Trip.K224Qrev	GCCCAGCTTCTCCTGGAGAATGCAGCCGC	81.0
CphAPstla	GCGTGCGGGCTGCAGGGATGTCGCTGAC	78.9
CphAPstlb	GTCAGCGACATCCCTGCAGCCCGCACGC	78.9